

Temperature dependence of exchange bias in polycrystalline ferromagnet-antiferromagnet bilayers

M. D. Stiles and R. D. McMichael

National Institute of Standards and Technology, Gaithersburg, MD 20899

(Accepted for publication in Physical Review B)

Contribution of the U. S. Government.

Not subject to U. S. copyright.

(M. D. Stiles, e-mail mark.stiles@nist.gov)

Abstract

We describe a simple model for the temperature dependence of the exchange bias and related effects that result from coupling a ferromagnetic thin film to a polycrystalline antiferromagnetic film. In this model, an important source of temperature dependence comes from thermal instabilities of the antiferromagnetic state in the antiferromagnetic grains, much as occurs in superparamagnetic grains. At low enough temperatures, the antiferromagnetic state in each grain is stable as the ferromagnetic magnetization is rotated and the model predicts the unidirectional anisotropy that gives rise to the observed exchange-bias loop shift. At higher temperatures, the antiferromagnetic state remains stable on short time scales, but on longer time scales, becomes unstable due to thermal excitations over energy barriers. For these temperatures, the model predicts the high field rotational hysteresis found in rotational torque experiments and the isotropic field shift found in ferromagnetic resonance measurements.

75.70.Cn,75.30.Gw,76.50.+g

I. INTRODUCTION

The response of a ferromagnetic thin film to applied fields can be changed by coupling it directly to an antiferromagnet. The most well known change is a shift of the hysteresis loop,¹ often called exchange bias. This loop shift is of interest in magnetic devices, because the coupling effectively “pins” the soft magnetic layers in the low fields used in devices.² Because these devices may be required to operate at temperatures on the order of 100 °C above room temperature or greater, the temperature dependence of exchange bias systems is quite important.

The coupling between the antiferromagnet and the ferromagnet leads to many other changes in the properties of exchange bias systems, which have been reviewed in Ref. 3. Rotational torque,^{4–7} ferromagnetic resonance,^{9–14} Brillouin light scattering,^{15,16} ac susceptibility,¹⁷ and anisotropic magnetoresistance¹⁸ have been used to measure the anisotropy of these systems. They all show the unidirectional anisotropy that gives rise to the hysteresis loop shift, but also show effects indicative of hysteretic processes as the ferromagnetic magnetization is rotated. Many of these measurements are done in fields large enough to saturate the ferromagnetic magnetization, indicating that the hysteretic processes must be occurring in the antiferromagnet. However, different techniques measure different aspects of these hysteretic processes.

In rotational torque measurements, the torque on a sample is measured as the sample is rotated in a magnetic field. In unbiased films, if the field is large enough to saturate the sample moment, then the magnetization follows the field reversibly. In this case, the torque integrates to zero when the sample is rotated through 360°. However, in exchange bias systems, the torque does not integrate to zero, even in very large applied fields.^{4–8} This behavior indicates that parts of the system are behaving irreversibly. When these parts of the system change configuration as the field is rotated, work is done and dissipated in the system. The high field rotational hysteresis is then the total work done on rotation of the magnetization through 360°.

Ferromagnetic resonance experiments¹⁴ on biased films relative to unbiased films show an isotropic shift of the resonance field superimposed on orientation-dependent shifts from other anisotropies. This shift can be modeled as coming from a rotatable anisotropy,^{19,20} an anisotropy that has a minimum that “follows” the steady state magnetization direction.

The unidirectional anisotropy, the high field rotational hysteresis, and the isotropic ferromagnetic resonance field shift can be explained in a single model which accounts for the thermal stability of the antiferromagnetic state on different times scales. This behavior is closely related to superparamagnetism. A superparamagnetic particle is in a well defined state when probed on short enough times scales, but not when probed on long enough time scales. The crossover between the two regimes depends strongly on temperature because the instability of the state arises from thermal transitions over some energy barrier. In our model, an analogous dependence on temperature and time scale exists in the finite and independent grains of the antiferromagnet.

For example, the apparently oxymoronic concept of a rotatable anisotropy is explained by the difference in behavior on different time scales. While the state of a part of the system may be stable on one time scale it may be unstable on a longer time scale. When we say that the state of a part of an antiferromagnetic grain is stable on some time scale, we mean that the sublattice magnetization direction is constant. Rotatable anisotropy is explained by the state of some of the antiferromagnetic grains being stable on the time scale of the microwave excitation, on the order of 10^{-9} s to 10^{-10} s, but being unstable on the time scale of measuring the ferromagnetic resonance signal at different field directions, on the order of 1 s to 10^2 s. As the ferromagnetic magnetization direction is rotated between different measurements, these grains that are unstable on the long time scale change states. These new states have energy minima that tend to be closer to the new magnetization direction than they would be in the absence of instability.^{13,14} This change in the directions of the minima associated with individual grains gives rise to the rotatable anisotropy.¹⁴ Thus, the isotropic field shift of the ferromagnetic resonance is determined by the the grains that change their state on the 1 to 10^2 s time scale.²¹

One difficulty with models for exchange-biased systems is that there are enough unknown properties to make it is possible to fit almost any model to any particular experimental result. To address this difficulty, it is important for models to predict the behavior of enough measurements, with as much variation as possible that the adjustable parameters be overconstrained rather than underconstrained. In a previous paper,²¹ we developed a model to describe both the unidirectional anisotropy and the hysteretic processes in polycrystalline exchange-bias systems. In this paper, we try to widen the predictions of our model by using it to predict the temperature dependence of the unidirectional anisotropy that leads to the loop shift, the isotropic field shift found in ferromagnetic resonance, and the high field rotational hysteresis found in rotational torque experiments.

II. MODEL

Our model for a polycrystalline exchange bias system consists of a ferromagnetic film coupled to independent antiferromagnetic grains.^{21,22} The ferromagnetic magnetization is assumed to be both saturated by and rotated by an external field. The antiferromagnetic grains are coupled to the ferromagnet by the direct exchange coupling between the interfacial spins of the ferromagnet and the interfacial spins of the antiferromagnetic grains. The coupling is frustrated to a large degree because, due to disorder at the interface, both sublattices of the antiferromagnet are present at the interface of each grain.²³ Statistical variations in the fraction occupied by each sublattice lead to a net coupling.^{24,25}

In a previous paper,²¹ we included spin flop coupling²⁶ at the interface. While simple estimates suggest that spin-flop coupling is strong in such systems,²⁶ and there is strong evidence for it in some systems,²⁷ it does not lead to a unidirectional anisotropy.^{21,28} In fact, spin-flop coupling reduces the unidirectional anisotropy that is due to coupling to the net moment of the antiferromagnet. We believe that the simple estimates of the importance of spin-flop coupling are not correct for the systems that have been investigated by ferromagnetic resonance and rotational torque and we do not include it in the present calculations.

For a more complete description of the interfacial coupling, see Ref. 21.

As the ferromagnetic magnetization direction, $\hat{\mathbf{M}}_{\text{FM}}$, is rotated, the magnetization direction near the interface, $\hat{\mathbf{m}}(0)$, in each antiferromagnetic grain adjusts itself to minimize the combination of the exchange energy at the interface and the partial domain wall energy^{23,29} in the antiferromagnet due to its deviation from its easy axis direction, $\hat{\mathbf{u}}$,

$$E_{\text{int}} = -NJ_{\text{net}}\hat{\mathbf{M}}_{\text{FM}} \cdot \hat{\mathbf{m}}(0) + \frac{Na^2\sigma}{2} [1 - \hat{\mathbf{m}}(0) \cdot (\pm\hat{\mathbf{u}})], \quad (1)$$

where N is the number of spins at the interface of that grain, a^2 is the area of the interface per spin, J_{net} is the effective interfacial coupling per spin for that grain, and σ is the domain wall energy per unit area in the antiferromagnet, which we assume has uniaxial anisotropy. The ferromagnetic magnetization is assumed to be saturated, so there is no partial domain wall in the ferromagnet.³⁰ While we will treat the case where the ferromagnetic magnetization, $\hat{\mathbf{M}}_{\text{FM}}$, is rotated in the interface plane, none of the unit vectors in Eq. (1), are restricted to lying in that plane. We choose to assign the antiferromagnetic magnetization direction, $\hat{\mathbf{m}}(0)$, to the direction of the sublattice magnetization for the sublattice that predominates at the interface. In the absence of coupling to the ferromagnet, there are two degenerate ground states in the antiferromagnet. One ground state has one sublattice magnetization along $\hat{\mathbf{u}}$ and the other has it along $-\hat{\mathbf{u}}$. These two ground states give two configurations that are local energy minima,²¹ one for each ground state of the uncoupled antiferromagnet

$$E^{(\pm)} = \frac{Na^2\sigma}{2} \left(1 - \left[1 + 2r\hat{\mathbf{M}}_{\text{FM}} \cdot (\pm\hat{\mathbf{u}}) + r^2 \right]^{1/2} \right), \quad (2)$$

where $r = 2J_{\text{net}}/\sigma a^2$, is the ratio of the direct coupling energy to half a domain wall energy. The minimum energy configurations have $\hat{\mathbf{m}}(0)$ lying in the plane defined by $\hat{\mathbf{u}}$ and $\hat{\mathbf{M}}_{\text{FM}}$.

In our model, the distributions of the characteristics of the antiferromagnetic grains are random. We assume that the distribution of easy axis orientations is isotropic, not only in the plane, but in all three dimensions, and that the distributions of the number of spins at the interface from each antiferromagnetic sublattice is statistical. The latter assumption leads to a distribution of effective interfacial coupling energies, $NJ_{\text{net}} = J_{\text{int}}|(N_1 - N_2)|$,

where N_1 and N_2 are the number of spins from each of the two sublattices exposed at the interface of that grain, where J_{int} is the interfacial exchange coupling strength for each spin pair. The absolute value comes from choosing the dominant sublattice for each grain as the reference sublattice for that grain. The assumptions, that N is large, and that N_1 and N_2 are statistically distributed, lead to a distribution of coupling strength ratios

$$\Phi(r, r_0) = \frac{2}{\pi r_0} \exp\left(-\frac{r^2}{\pi r_0^2}\right), \quad (3)$$

where the mean value is

$$r_0 = \frac{2J_{\text{int}}}{\sigma a^2} \sqrt{\frac{2}{\pi N}}. \quad (4)$$

In real samples, the grain size N will also be distributed in some way. For clarity, we compute the behavior for different grain sizes rather than averaging over a distribution.

We consider exchange bias systems in which the Curie temperature of the ferromagnet is much greater than the Néel temperature of the antiferromagnet, which is usually, but not always,³¹ the case. Thus, we assume that the properties of the ferromagnet are temperature independent. Also, since the proximity of the ferromagnet is likely to induce a moment in the antiferromagnet close to the interface, we assume that the coupling at the interface is also temperature independent. We include two contributions to the temperature dependence. The first source of temperature dependence that we include in the model is the domain wall energy in the antiferromagnet. We assume that $\sigma = \sigma_0(1 - T/T_N)^{5/6}$, where T_N is the Néel temperature, based on $\sigma \propto \sqrt{A_{\text{AF}}K_{\text{AF}}}$, and the approximations that the antiferromagnetic moment $m_{\text{AF}} \propto (T_N - T)^{1/3}$, the anisotropy constant, $K_{\text{AF}} \propto m_{\text{AF}}^3$ for uniaxial anisotropy,³² and the exchange stiffness constant $A_{\text{AF}} \propto m_{\text{AF}}^2$ as indicated approximately by analogy to spin-wave dispersions in some ferromagnets.³³ This approximation is crude, but gives a simple form for the temperature dependence such that domain walls become easy to create as the Néel temperature is approached.

The second source of temperature dependence in our model is analogous to superparamagnetism³⁴ in small ferromagnetic particles. We assume that for certain temperatures, thermal fluctuations can lead to switching of the antiferromagnetic state in the

grains.²² Two differences between our model and the standard models for superparamagnetism are 1) we consider antiferromagnetic grains, which only couple weakly to external magnetic fields (we assume no coupling), and 2) we assume that the columnar grains are longer than domain walls in the antiferromagnet. This means that the mechanism for switching the state of the grains is domain wall nucleation and motion, rather than coherent rotation. This assumption is clearly only appropriate for grains larger than a certain size. For smaller grains, a coherent rotation model could be used.²²

We assume that the antiferromagnetic order on short time scales sets in at the bulk Néel temperature, but that it can be thermally switched in the finite-sized grains on some longer time scale. In this paper, we assume that this switching is slow compared to the inverse of the ferromagnetic resonance frequencies and depending on the temperature, the switching is either fast or slow compared to measurement times. For small enough grains, there may be a temperature range in which the switching is even fast on the time scale of ferromagnetic resonance. In this case, which we have not treated, we expect the switching to contribute to an increase in the resonance linewidth.

There is a great deal of evidence for relaxation on laboratory time scales in exchange-bias systems. Early measurements showed a training effect,⁶ in which the hysteresis loop changes as it is cycled repeatedly. More recent measurements³⁵ show that if the sample is held with the ferromagnetic magnetization in the hard direction of the unidirectional anisotropy, the size of the bias decreases with a time scale on the order of hours. Furthermore, as the temperature is increased, the time constant decreases.

To determine the thermal switching rate, we make a simple model for the barrier between the two states described by Eq. (2). This model is based on a picture in which switching nucleates at the interface and proceeds by propagation of a domain wall out the other end of the antiferromagnetic grain. In this picture the “barrier state” consists of the final state plus a domain wall far from the interface. The energy of this state is an estimate of the true barrier energy. Thus, starting from the (+) state, the barrier to the (−) state is

$$\Delta E = \frac{Na^2\sigma}{2} \left([1 + 2r\hat{\mathbf{M}}_{\text{FM}} \cdot \hat{\mathbf{u}} + r^2]^{1/2} - [1 - 2r\hat{\mathbf{M}}_{\text{FM}} \cdot \hat{\mathbf{u}} + r^2]^{1/2} \right) + Na^2\sigma. \quad (5)$$

A more realistic model for the barrier would require a very detailed simulation of the switching of a grain. The simple model we have chosen has several features we expect of a more realistic model. The energy scale is set by the domain wall energy in the antiferromagnet, which is appropriate for grains larger than a domain wall length. Also, the barrier is higher for states which have more favorable coupling to the ferromagnet.

At a temperature T , the probability of remaining in an initial state for a period of time t is

$$P(t) = \exp[-\nu t \exp(-\Delta E/k_{\text{B}}T)]. \quad (6)$$

For $\nu t = 10^9 \text{ s}^{-1} \times 1 \text{ s}$ and several values of $Na^2\sigma/k_{\text{B}}T$, this probability is shown in Fig. 1 as a function of the in-plane rotation angle of the magnetization, ϕ . For most parameter choices, the probability is close to one for a range of angles and then makes a rapid transition to close to zero for other angles. These rapid transitions suggest the further approximation that this probability be chosen to be either zero or one with the border between the two regimes given by

$$\Delta E/k_{\text{B}}T = \log \nu t \approx 20 \quad (7)$$

Thus, if $\Delta E > 20k_{\text{B}}T$, the grain is assumed to be stable in the initial state, and if $\Delta E < 20k_{\text{B}}T$ it is unstable. If the barrier from the other state, $2Na^2\sigma - \Delta E < 20k_{\text{B}}T$ as well, then the grain is unstable in both states.

Approximating the state of each grain as either stable or unstable is closely related to the critical angle description of instability described in Ref. 21. That paper described zero temperature instability due to the barrier going to zero when a partial domain wall is wound up past a certain angle in the antiferromagnet. The instability at the critical angle leads to switching behavior similar to that described here. In this paper, there are several differences. Here, the model chosen for the barrier is always non-negative, so there

is essentially no instability at $T = 0$. In addition, the model used here allows instability in both states. This means that on the time scale of the measurement, $t \approx 1$ s, some grains flip between both states, occupying both with appropriate thermal probabilities.

Other models for the barrier can be treated in a straightforward extension of the results presented in this paper. The difficulty is determining sensible models. In some systems there will be grains with energy barriers that go to zero for some directions of the magnetization, as described in our previous paper.²¹ In this case, the effect of instabilities described below will persist down to $T = 0$ K. In the model of the present paper, where essentially all energy barriers are finite, all grains become stable at $T = 0$ K.

In the approximation used in this paper, we classify grains as either stable, partially stable, or unstable as a function of temperature and applied field direction. A stable grain has large enough barriers from both the (+) and (−) states that it will remain in either state on the time scale of the measurement. An unstable grain has small enough barriers from both states that the state will flip from one state to the other on a time scale fast compared to the measurement time. A partially stable grain will stay in one state, but not the other. For a particular grain, the different regions of this behavior are illustrated in Fig. 2.

At low enough temperatures, the grain is stable in either state for all magnetization angles. If the antiferromagnetic order is set in the presence of a particular magnetization direction, this grain will contribute to the unidirectional anisotropy that gives rise to the loop shift.

At intermediate temperatures, the grain goes through regions of stability and regions of partial stability as the magnetization is rotated. Both states of the grain become unstable for particular field directions. As the magnetization is rotated, the grain will reach the point of instability and the state of the grain will switch. Since the grain “forgets” its initial state when it switches, it ceases to contribute to the unidirectional anisotropy, but instead contributes to the rotatable anisotropy. For angles where the grain is stable, it contributes an anisotropy that has a minimum in one direction. When it switches between states, it favors one of two (opposite) directions depending on the direction of the magnetization and

its history. Since the state switches to a state that is lower in energy, the grain, on average, has an energy minimum closer to the direction of the magnetization than in the absence of switching. This leads to an anisotropy that “follows” the magnetization, a rotatable anisotropy. In addition, a finite energy is dissipated when the state of the grain switches. This energy dissipation makes a contribution to the high field rotational hysteresis equal to the difference in energy between the two states when one state becomes unstable.

At higher temperatures, the magnetization angles at which the states become unstable approach each other and eventually cross. Now, the grain goes through regions of partial stability and regions of instability. At this point, no energy is dissipated as the magnetization is rotated. In regions of instability, the two states are in thermal equilibrium. In regions of partial stability, only one state is stable. Therefore, the energy of the system is a single-valued function of the magnetization direction, so the magnetization is rotated reversibly, and there is no contribution to the high field rotational hysteresis. There is still a contribution to the rotatable anisotropy, because the state that is lower in energy has a greater thermal weight. At still higher temperature, the grain is unstable for all magnetization directions, but still contributes to the rotatable anisotropy.

As the temperature increases further, the domain wall energy decreases and goes to zero at the Néel temperature. Thus, the value of $k_B T / Na^2 \sigma$, the y -axis in Fig. 2, increases faster than linearly with temperature.

Starting from high temperature and going to low temperatures, the behavior described above can be understood in terms of kinetic barriers to establishing equilibrium. At high temperatures, but still below the Néel temperature, each antiferromagnetic grain is in a well-defined state on short times scales, but on longer time scales, there is thermal equilibrium between the two possible states. As the temperature is lowered, the kinetic barrier between the two states increases, and the time it takes to establish equilibrium increases. Eventually, this time becomes comparable to the measurement time scale, and the grain becomes stable in the state it was in when the equilibration time became greater than the measurement time.

The contributions to the unidirectional anisotropy and the rotatable anisotropy are determined from the curvature of the energy surface as a function of the angle of the magnetization.^{14,21} We consider a sample with a steady-state ferromagnetic magnetization in the (1,0,0) direction and consider small deviations around that direction. The curvature of the energy with respect to these deviations then determines the effective anisotropies induced in the ferromagnet by the coupling to the antiferromagnet. For a grain with an easy axis in the direction $(\sin \theta_{\mathbf{u}} \cos \phi_{\mathbf{u}}, \sin \theta_{\mathbf{u}} \sin \phi_{\mathbf{u}}, \cos \theta_{\mathbf{u}})$, and a magnetization near the (1,0,0) direction given by $(\cos \epsilon \cos \delta, \sin \epsilon \sin \delta, \sin \epsilon)$, where ϵ and δ are the small angles associated with the microwave excitation, the angle between the magnetization and the easy axis is determined by

$$\hat{\mathbf{M}}_{\text{FM}} \cdot \hat{\mathbf{u}} \approx \sin \theta_{\mathbf{u}} \cos \phi_{\mathbf{u}} + \delta \sin \theta_{\mathbf{u}} \sin \phi_{\mathbf{u}} + \epsilon \cos \theta_{\mathbf{u}} - \frac{\epsilon^2 + \delta^2}{2} \sin \theta_{\mathbf{u}} \cos \phi_{\mathbf{u}}. \quad (8)$$

This quantity enters the energy, Eq. (2). To determine the appropriate curvatures, differentiate the energy and weight the two minima by their occupation probability, and take the limit that δ and ϵ go to zero.

We assume that the occupation probability of a state is independent of ϵ and δ because the microwave excitation occurs on a time scale fast compared to changes in occupation. Then, the second derivative of the free energy with respect to ϵ is

$$\frac{d^2 F}{d\epsilon^2} = P^{(+)} \frac{d^2 E^{(+)}}{d\epsilon^2} + P^{(-)} \frac{d^2 E^{(-)}}{d\epsilon^2}, \quad (9)$$

where $P^{(\pm)}$ is the probability of being in the respective state. Similar forms hold for the second derivative with respect to δ and the cross term. If one state of the grain is stable, the probability of being in a state is either zero or one. If both states are unstable, the probabilities are given by the thermal occupation probabilities

$$P^{(\pm)} = \frac{e^{-\beta E^{(\pm)}}}{e^{-\beta E^{(+)}} + e^{-\beta E^{(-)}}}, \quad (10)$$

where we have $\beta = 1/k_{\text{B}}T$

From the energy surface curvatures and the work done when switching, we compute the unidirectional anisotropy, the rotatable anisotropy, and the high field rotational hysteresis by

averaging over the assumed distributions of grain orientations and interfacial net moments. As a function of temperature, we first determine the domain wall energy in the antiferromagnet. From that we determine the distribution of the ratio between the interfacial coupling and the domain wall energy. Then we numerically integrate over the distributions to determine the quantities of interest. The averaged curvatures are related to the appropriate anisotropies by computing the size of the anisotropy that gives the same curvature.

III. RESULTS

If we assume that all of the grains are stable; i.e. there are no thermally induced changes in configuration, then the rotatable anisotropy and the high field rotational hysteresis are both zero. The temperature dependence of the unidirectional anisotropy, σ_{ex} , comes from the temperature dependence of the domain wall energy. Its value is found by integrating the contribution for a particular value of the parameter r , given in Ref. 21, over the distribution of values, Φ , given in Eq. (3)

$$Eq. (3)\sigma_{\text{ex}} = \frac{\sigma_0}{2} \left(\frac{T_N - T}{T_N} \right)^{5/6} \int_0^\infty dr \Phi \left(r, r_0 \left(\frac{T_N - T}{T_N} \right)^{-5/6} \right) F_1(r), \quad (11)$$

where we have

$$F_1(r) = \begin{cases} \frac{r}{2} \left(1 - \frac{r^2}{5} \right) & r < 1 \\ \frac{1}{2} \left(1 - \frac{1}{5r^2} \right) & r > 1 \end{cases}, \quad (12)$$

and r_0 defined in Eq. (4). The behavior is illustrated in Fig. 3 for several values of the ratio of r_0 .

The parameter, r_0 , is one of the two dimensionless parameters that characterize the model. It is the ratio of the average interfacial coupling to the domain wall energy at zero temperature. As seen in Fig. 3, it determines the saturation of the bias at low temperatures. Once the domain wall energy becomes greater than typical interfacial coupling energies, this bias saturates. If the zero temperature wall energy is lower than the interfacial coupling energy, the unidirectional anisotropy will continue to increase as the temperature is lowered.

When thermal instability in the grains, as modeled by the barriers in Eq. (5), is included in the model, the other dimensionless parameter of importance is

$$b = \frac{Na^2\sigma_0}{kT_N}. \quad (13)$$

This parameter is the ratio of the domain wall energy (times the area of the grain) divided by the thermal energy at the Néel temperature. When this ratio is large, the different states of the grain become stable very quickly as the temperature is lowered below the Néel temperature. When b is small, the grain does not contribute to the unidirectional anisotropy until significantly below the Néel temperature. As seen in Fig. 4, this parameter largely determines the reduction of the blocking temperature compared to the Néel temperature. In this model, this reduction comes about from the analogy of the behavior of the antiferromagnetic grains to superparamagnetism. Grains smaller than a certain size are thermally unstable until below the blocking temperature.

In addition to the reduction of the blocking temperature as the parameter b decreases, and the saturation of the unidirectional anisotropy as r_0 decreases, Fig. 4 shows several other interesting features. First, the rotatable anisotropy becomes non-zero at the Néel temperature, above the blocking temperature. All grains contribute to the rotatable anisotropy. As the temperature decreases, the rotatable anisotropy increases with the increasing domain wall energy until the blocking temperature. Then, as grains become stable they start contributing to the unidirectional anisotropy and not to the rotatable anisotropy. The rotatable anisotropy decreases. In this model, in which all the energy barriers are non-negative, all grains are stable at $T = 0$, and the rotatable anisotropy goes to zero.

Only grains that are partially stable contribute to the high field rotational hysteresis. Thus, this quantity is also zero above the blocking temperature. It increases as the temperature is lowered because the increasing stability of the grains allows them to be wound up further in the energetically unfavored state. More energy is dissipated when the grain switches state. Eventually, the grains become stable, and the high field rotational hysteresis goes to zero at $T = 0$.

The temperature dependence of the unidirectional anisotropy shown in Fig. 4 for various parameters spans the range of what is seen experimentally. While a set of parameters can be chosen to agree with any particular experiment, especially if a distribution of grain sizes is assumed, such agreement is not very satisfactory. However, the predictions of the temperature dependence of the high field rotational hysteresis and the rotatable anisotropy should constrain the model significantly when these results become available and lead to a much more satisfactory test of the model.

A distribution of grain sizes and hence blocking temperatures can explain the “memory” effects found in some systems.³⁶ If there is a distribution of blocking temperatures, each grain will start to contribute to the unidirectional anisotropy at a different temperature. If the ferromagnetic magnetization is changed as the sample is cooled, different grains will contribute to unidirectional anisotropies in different directions. It would be interesting to measure the rotatable anisotropy or the high field rotational hysteresis on these samples to see if they are consistent with a distribution of blocking temperatures. If there are blocking temperatures very close to zero temperature, the rotatable anisotropy should persist to zero temperature.

One point that deserves to be discussed is the general agreement between experimental results on polycrystalline and single crystal samples, and what aspects of this model might apply to single crystal samples. In some single crystal samples,^{27,37} there is evidence for the importance of the motion of domain walls that are perpendicular to the sample and move in the sample plane. At high temperatures, these domain walls can be mobile on long time scales and fixed on short time scales. As the temperature decreases, the pinning of the domain walls becomes more important and the domain walls only move on much longer time scales. The motion and thermal pinning and unpinning of domain walls perpendicular to the interface are more complicated than the model we have treated for the motion of domain walls in independent grains. However, in both cases there are regions of the antiferromagnet that are unstable due to domain wall motion through those regions. This similarity may account for the general agreement found in experimental studies of these systems.

IV. SUMMARY

In this paper, we describe a model for the temperature dependence of polycrystalline exchange-bias systems. The predictions of this model should prove useful when measurements of the temperature dependence of several properties of the same samples become available. The temperature dependence comes from that of the domain wall energy in the antiferromagnetic grains and from thermally activated switching of the antiferromagnetic grains. These latter processes are analogous to superparamagnetism in small ferromagnetic particles. Assuming a isotropic distribution of easy axis directions, and a statistical distribution of the net moment at the interface of the grains, we compute the unidirectional anisotropy that gives rise to the loop shift, a rotatable anisotropy that gives rise to an isotropic shift of the resonance field, and a rotational hysteresis measured in torque experiments in high field.

The thermal activation of the switching causes there to be a blocking temperature that is below the Néel temperature. Above this temperature, the antiferromagnetic order in the grains is not stable and no unidirectional anisotropy develops. On the time scale of the resonance frequency in ferromagnetic resonance measurements, the order is stable. Thus the coupling to the antiferromagnetic grains gives rise to an effective anisotropy for the ferromagnet that rotates as the ferromagnetic magnetization is rotated on a measurement time scale of order 1 s. Below the blocking temperature, the antiferromagnetic order first becomes stable in one configuration, but not the other. For these grains, the antiferromagnetic order is no longer a single valued function of the ferromagnetic magnetization directions, but depends on its history. The energy dissipated gives rise to the high field rotational hysteresis. At lower temperatures, the antiferromagnetic order becomes stable, and the grains contribute to the unidirectional anisotropy and not the rotatable anisotropy or the high field rotational hysteresis.

The saturation of the unidirectional anisotropy at low temperatures is determined by the ratio of the average interfacial coupling energy to the zero temperature domain wall

energy. If the domain wall energy is the smaller of the two, it determines the size of the unidirectional anisotropy. If the interfacial coupling energy is the smaller of the two, it determines the unidirectional anisotropy, which saturates at low temperature due to the assumed temperature independence of the interfacial coupling at low temperatures.

REFERENCES

- ¹ W. H. Meiklejohn and C. P. Bean, Phys. Rev. **102**, 1413 (1956).
- ² B. Dieny, V. S. Speriosu, S. Metin, S. S. P. Parkin, B. A. Gurney, P. Baumgart, and D. R. Wilhoit, J. Appl. Phys. **69**, 4774 (1991).
- ³ J. Nogués and I. K. Schuller, J. Magn. Magn. Mater. **192**, 203 (1999).
- ⁴ W. H. Meiklejohn, J. Appl. Phys. **33**, 1328 (1962).
- ⁵ D. Paccard, C. Schlenker, O. Massenet, R. Montmory, and A. Yelon, Phys. Stat. Sol. **16**, 301 (1966).
- ⁶ C. Schlenker, J. de Phys. Coll. **C 2**, 157 (1968).
- ⁷ C.-H. Lai, H. Matsuyama, R. L. White, T. C. Anthony, And G. G. Bush, J. Appl. Phys. **79**, 6389 (1996).
- ⁸ C. Schlenker, S. S. P. Parkin, J. C. Scott, and K. Howard, J. Magn. Magn. Mater. **54-57**, 801 (1986).
- ⁹ J. C. Scott, J. Appl. Phys., **57**, 3681 (1985).
- ¹⁰ W. Stoecklein, S. S. P. Parkin, and J. C. Scott, Phys. Rev. B, **38**, 6847 (1988).
- ¹¹ A. Layadi, W. C. Cain, J.-W. Lee and J. O. Artman, IEEE Trans. Mag., **23**, 2993 (1987).
- ¹² R. D. McMichael, W. F. Egelhoff, Jr., and L. H. Bennett, IEEE Trans. Mag., **31**, 3930 (1995).
- ¹³ P. Lubitz, J. J. Krebs, M. M. Miller, and S. Cheng, J. Appl. Phys., **83**, 6819 (1998).
- ¹⁴ R. D. McMichael, M. D. Stiles, P. J. Chen, and W. F. Egelhoff, Jr., Phys. Rev. B **58**, 8605 (1998); R. D. McMichael, M. D. Stiles, P. J. Chen, and W. F. Egelhoff, Jr., J. Appl. Phys., **83**, 7037 (1998).

- ¹⁵ A. Ercole, T. Fujimoto, M. Patel, C. Daboo, R. J. Hicken, and J. A. C. Bland, *J. Magn. Magn. Mater.* **156** 121 (1996).
- ¹⁶ P. Miltényi, M. Gruyters, G. Güntherodt, J. Nogués, I. K. Schuller, *Phys. Rev. B* **59**, 3333 (1999).
- ¹⁷ V. Ström, B. J. Jönsson, K. V. Rao, and Dan Dahlberg, *J. Appl. Phys.* **81**, 5003 (1997).
- ¹⁸ B. H. Miller and E. Dan Dahlberg, *Appl. Phys. Lett* **69**, 3932 (1996).
- ¹⁹ R. J. Prosen, J. O. Holmen, and B. E. Gran, *J. Appl. Phys.*, **32**, 91S (1961).
- ²⁰ J. M. Lommel and C. D. Graham, Jr., *J. Appl. Phys.*, **33**, 1160 (1962).
- ²¹ M.D. Stiles, and R.D. McMichael, *Phys. Rev. B* **59**, 3722 (1999).
- ²² E. Fulcomer and S. H. Charap, *J. Appl. Phys.* **43**, 4190 (1972).
- ²³ L. Néel, *Ann. Phys. (Paris)* **2**, 61 (1967). An English translation is available, in “Selected Works of Louis Néel,” ed. N. Kurti, Gordon and Breach Science Publishers, (New York, 1988), p. 469.
- ²⁴ A. P. Malozemoff, *Phys. Rev. B* **35**, 3679 (1987); *J. Appl. Phys.* **63**, 3874 (1988).
- ²⁵ K. Takano, R. H. Kodama, A. E. Berkowitz, W. Cao, and G. Thomas, *Phys. Rev. Lett.* **79**, 1130 (1997).
- ²⁶ N. C. Koon, *Phys. Rev. Lett.* **78**, 4865 (1997).
- ²⁷ Y. Ijiri, J. A. Borchers, R. W. Erwin, S.-H. Lee, P. J. van der Zaag, and R. M. Wolf, *Phys. Rev. Lett.* **80**, 608 (1998).
- ²⁸ T. C. Schulthess and W. H. Butler, *Phys. Rev. Lett.* **81**, 4516 (1998).
- ²⁹ D. Mauri, H. C. Siegmann, P. S. Bagus, and E. Kay, *J. Appl. Phys.* **62**, 3047 (1987).
- ³⁰ S. S. P. Parkin, V.R. Deline, R. O. Hilleke, and G. P. Felcher, *Phys. Rev. B* **42**, 10583

(1990).

³¹ X. W. Wu and C. L. Chien, Phys. Rev. Lett. **81**, 2795 (1998).

³² See S. V. Vonsovskii, *Magnetism* v. 2 (John Wiley & Sons, New York 1974) p. 946 and references therein.

³³ M. B. Stearns, in *Landolt-Börnstein New Series III/19a* (Springer Verlag, Berlin 1986) p. 72-81 and references therein.

³⁴ J. D. Livingston and C. P. Bean, J. Appl. Phys. **32** 1964 (1961).

³⁵ P. A. A. van der Heijden, T. F. M. M. Maas, W. J. M. de Jonge, J. C. S. Kools, F. Roozeboom, and P. J. van der Zaag, Appl. Phys. Lett. **72**, 492 (1998); P. A. A. van der Heijden, T. F. M. M. Maas, J. C. S. Kools, F. Roozeboom, P. J. van der Zaag, and W. J. M. de Jonge, J. Appl. Phys. **83**, 7201 (1998).

³⁶ N. J. Gökemeijer and C. L. Chien, J. Appl. Phys. **85**, 5516 (1999).

³⁷ V. I. Nikitenko, V. S. Gornakov, L. M. Dedukh, Yu. P. Kabanov, A. F. Khapitov, A. J. Shapiro, R. D. Shull, A Chaiken, and R. P. Michel, Phys. Rev. B **57**, R8111 (1998).

FIGURES

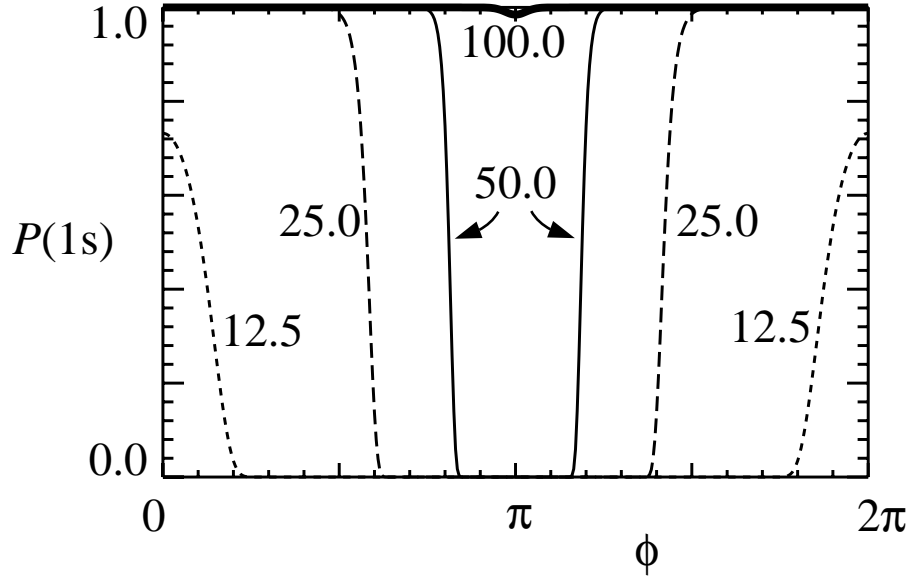


FIG. 1. Probability for the order of an antiferromagnetic grain to remain in a particular state for $t = 1s$ as a function of angle as the magnetic field is rotated around (0,0,1). The different curves are for different values of $Na^2\sigma/k_B T$, 100.0 (heavy solid line), 50.0 (solid line), 25.0 (dashed line), and 12.5 (dotted line). For this grain, the ratio $r = 1.0$, and the easy axis is in the (0.9, 0.0, 0.44) direction.

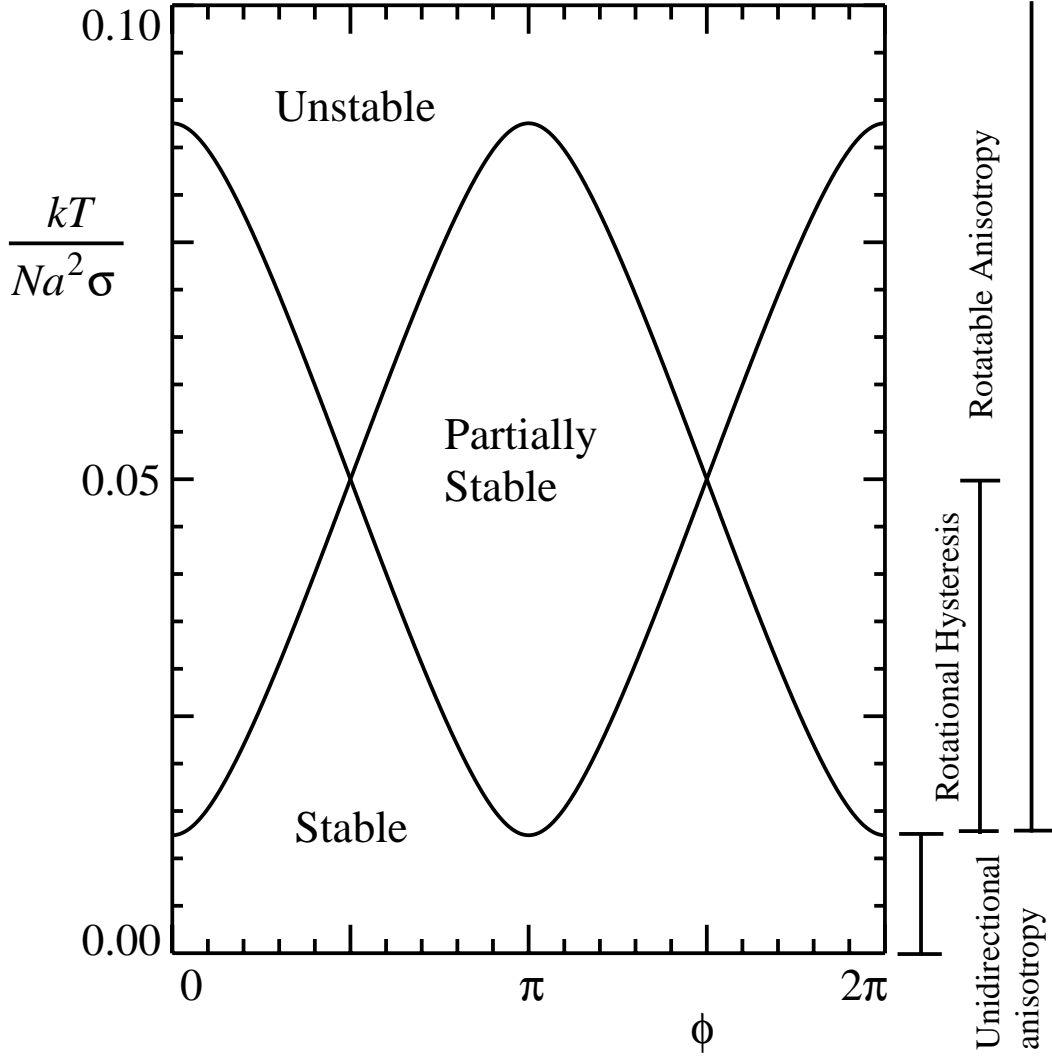


FIG. 2. Stability of order in an antiferromagnetic grain as a function of magnetic field angle and the ratio of temperature to domain wall energy. At each angle there are two configurations for the antiferromagnetic order. At low temperature, the order is stable in both states (stable), at high temperature in neither state (unstable), and at intermediate temperatures stable in one state or the other depending on field angle (partially stable). Bars to the right of the plot show the temperature ranges over which this grain contributes to different processes. The parameters for this grain are the same as in Fig. 1.

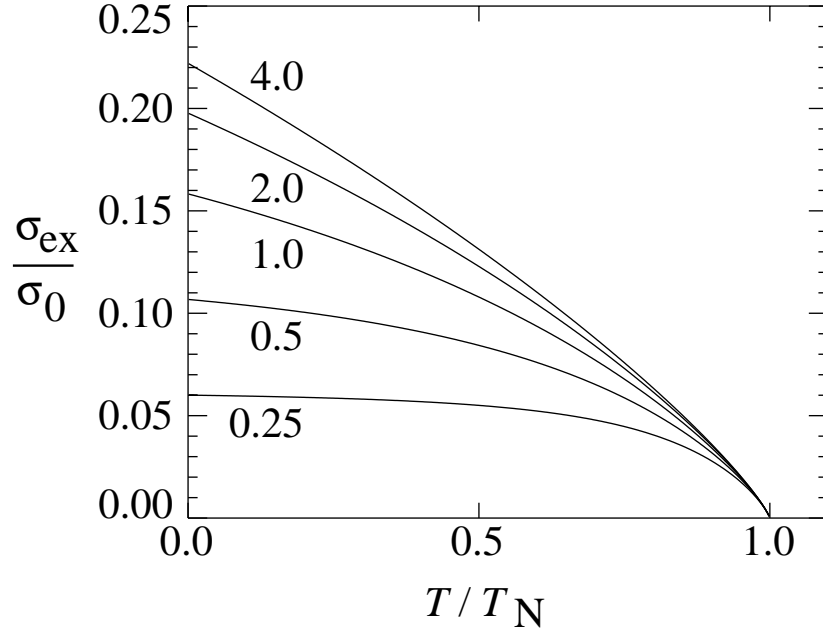


FIG. 3. Unidirectional anisotropy as a function of temperature assuming all grains are stable. The various curves are labeled by different values of the dimensionless parameter, r_0 (see Eq. (4)).

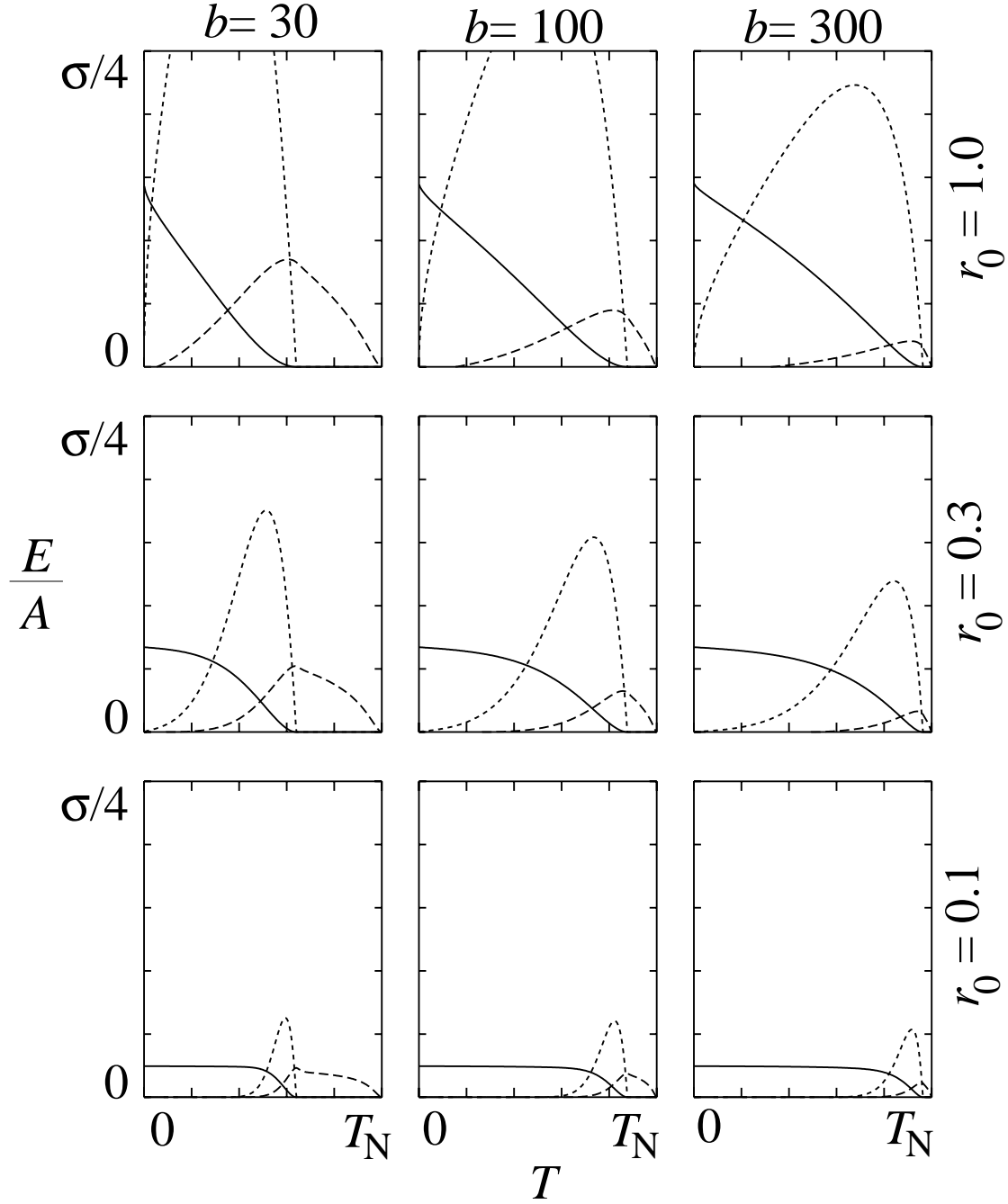


FIG. 4. The temperature dependence of the unidirectional anisotropy (solid lines), rotatable anisotropy (dashed lines), and rotational hysteresis (dotted lines), each an energy per area (E/A) in units of the domain wall energy σ for various values of the dimensionless parameters, r_0 and b (See Eqs. (4) and (13)).